ANNALS OF GEOPHYSICS, 69, 6, 2026; doi:10.4401/ag-9564
OPEN ACCESS

SUPPLEMENTARY MATERIAL TO

ENHANCING RESOLUTION IN LOCAL PASSIVE SEISMIC TOMOGRAPHY: ADAPTIVE GRID IMPLEMENTATION AT AGUNG VOLCANO, INDONESIA

I Putu Raditya Ambara Putra[1], David Prambudi Sahara[2], Wahyu Hidayat[1], Sri Widiyantoro[2], Andri Dian Nugraha[2]

[1] Geophysical Engineering, Faculty of Technology Mineral and Energy, UPN Veteran Yogyakarta, Yogyakarta 55283, Indonesia
[2] Global Geophysics Research Group, Faculty of Mining and Petroleum Engineering, Institut Teknologi Bandung, Bandung 40132, Indonesia

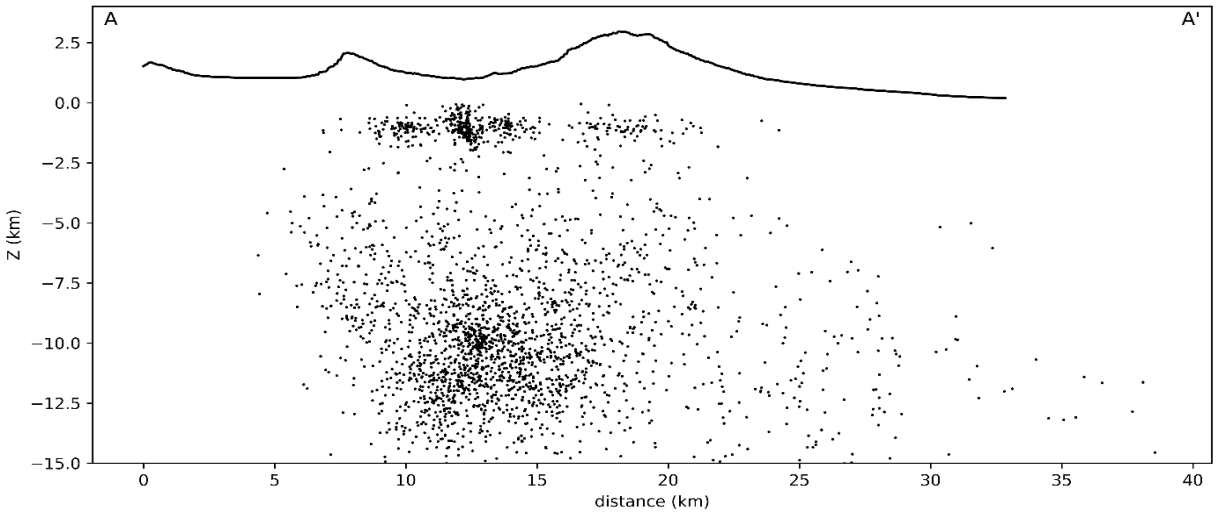


Figure S1. Cross-section A-A′ showing the distribution of hypocenter data (Sahara et al., 2021) used in this study.

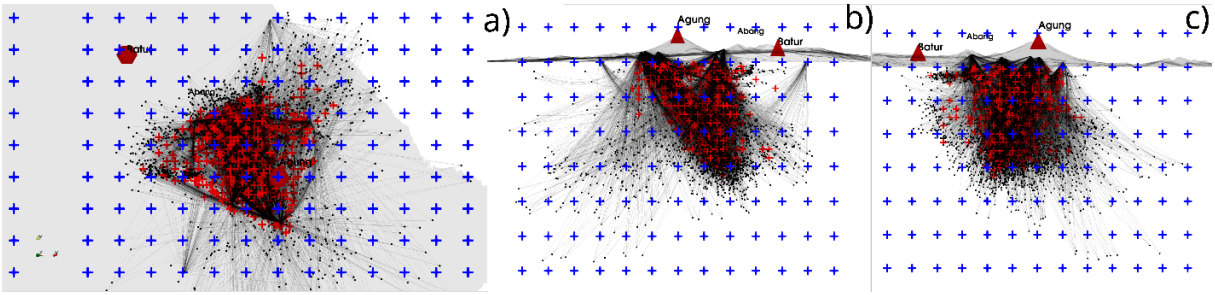


Figure S2. The position of nodes used to construct the Voronoi grid before (blue '+') and after (red '+') applying the adaptive scheme in CKB synthetic test. (a) map view, (b) looking to west, (c) looking to north.

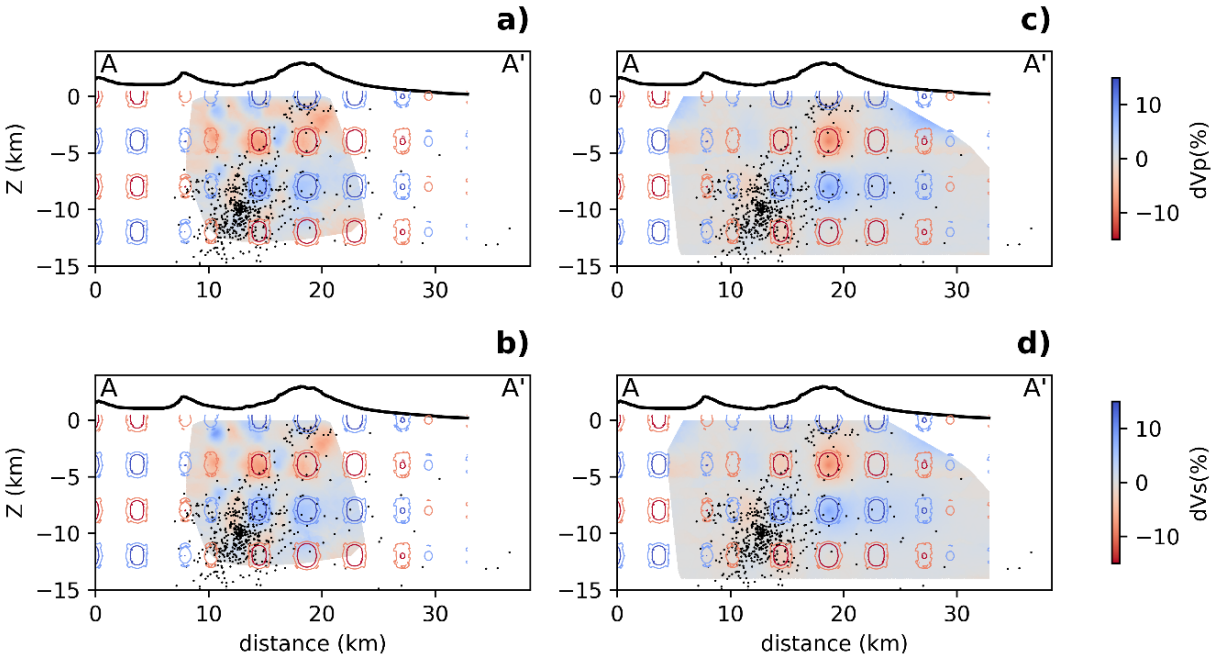


Figure S3. Results of the CKB synthetic test (1% noise) for the adaptive grid scheme (a and b) and the fixed grid scheme (c and d), for the parameters dVp (a and c) and dVs (b and d) respectively. The contour lines in each figure represent the synthetic checkerboard model used as a reference, with red indicating negative anomalies and blue indicating positive anomalies.

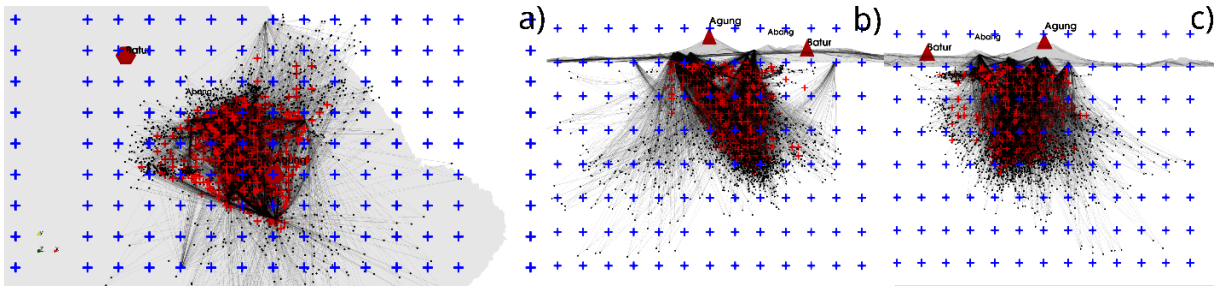


Figure S4. The position of nodes used to construct the Voronoi grid before (blue '+') and after (red '+') applying the adaptive scheme in Shifted CKB synthetic test. (a) map view, (b) looking to west, (c) looking to north.

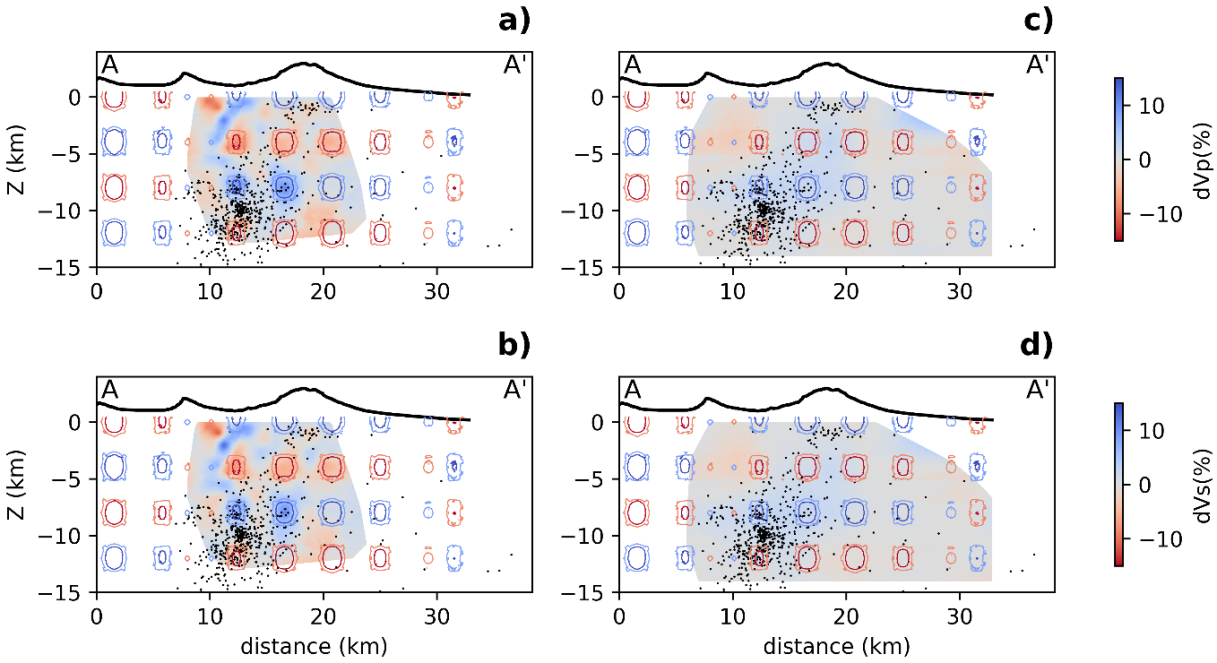


Figure S5. Results of the Shifted CKB synthetic test (1% noise) for the adaptive grid scheme (a and b) and the fixed grid scheme (c and d), for the parameters dVp (a and c) and dVs (b and d) respectively. The contour lines in each figure represent the synthetic checkerboard model used as a reference, with red indicating negative anomalies and blue indicating positive anomalies.

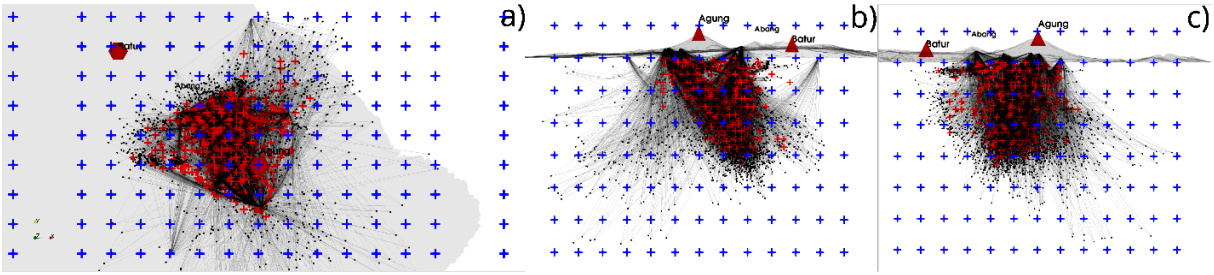


Figure S6. The position of nodes used to construct the Voronoi grid before (blue '+') and after (red '+') applying the adaptive scheme in low-velocity block synthetic test. (a) map view, (b) looking to west, (c) looking to north.

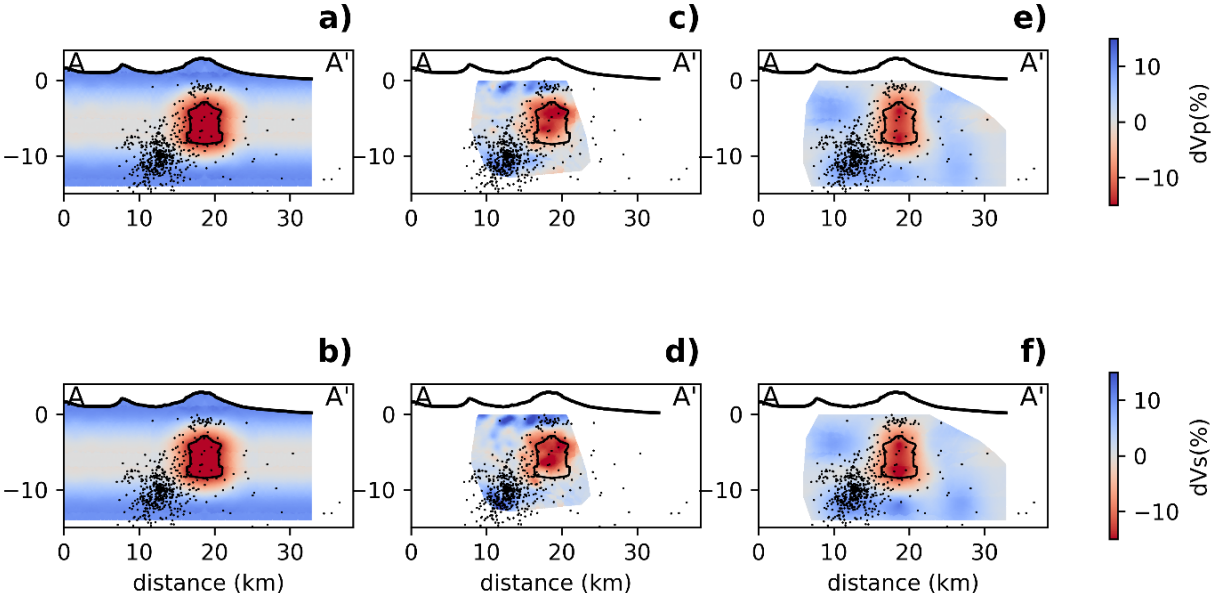


Figure S7. Synthetic test results for the low-velocity block model (1% noise). (a) and (b) show the synthetic dVp and dVs models, (c) and (d) show the results of the dVp and dVs inversions using an adaptive grid scheme, (e) and (f) show the results of the dVp and dVs inversions using a fixed grid scheme.

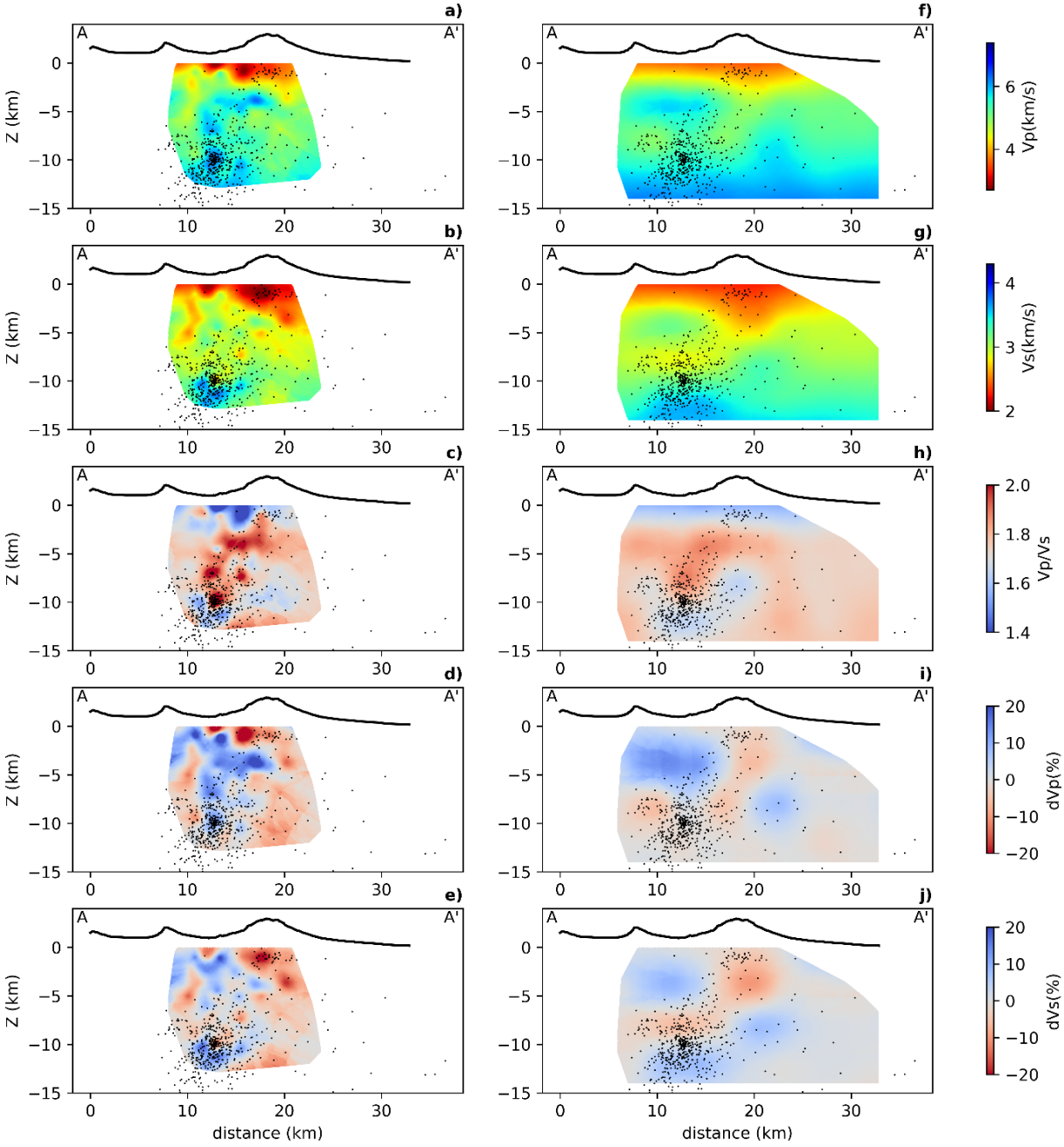


Figure S8. Results of synthetic tests on a complex model (1% noise) showing the parameters Vp, Vs, Vp/Vs, dVp and dVs, respectively, for the adaptive grid scheme (a-e) and the fixed grid scheme (f-j).

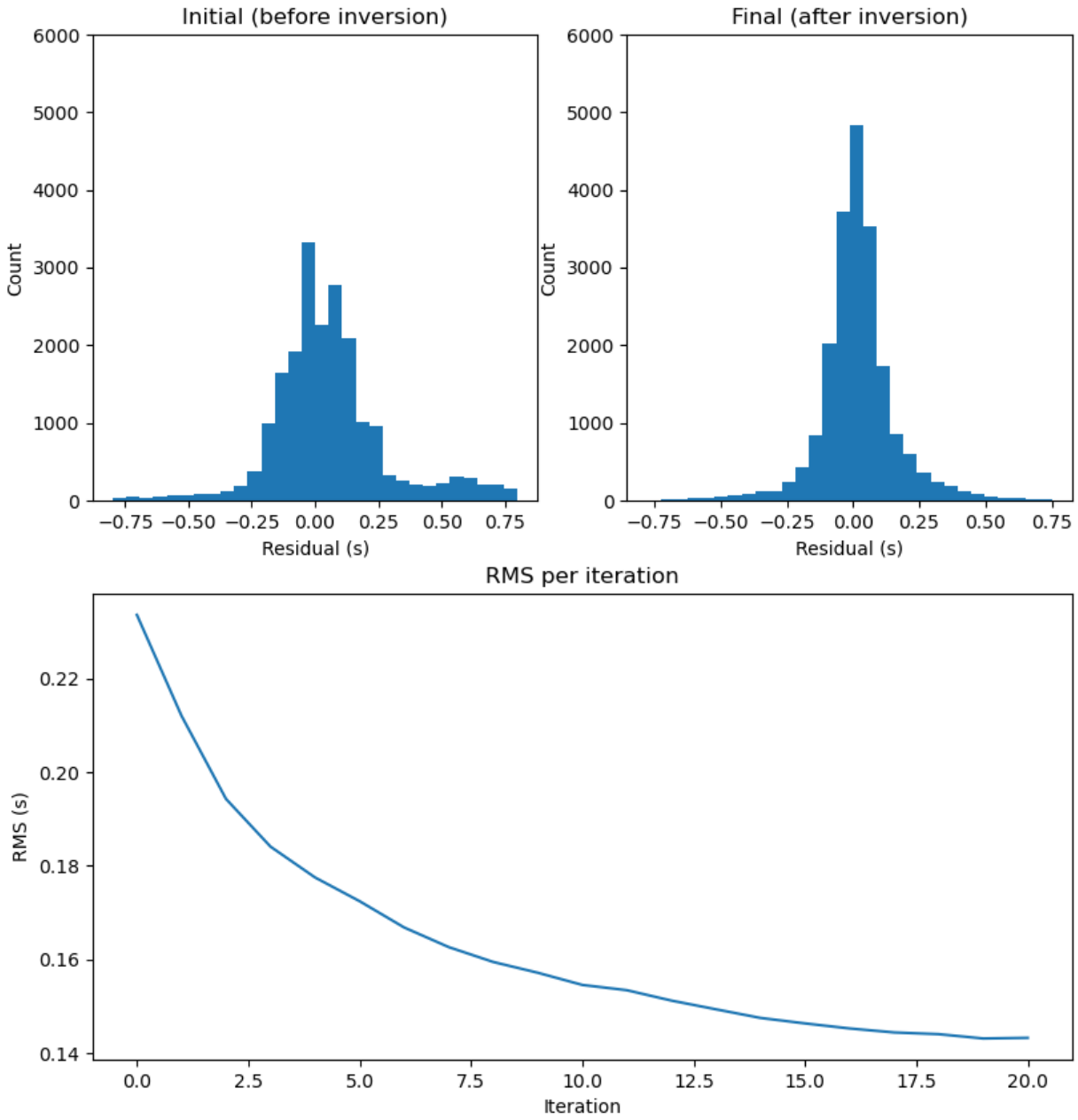


Figure S9. A comparison of the residual RMS distribution before and after tomographic inversion (top) and the convergence trend of the residual RMS per iteration (bottom).

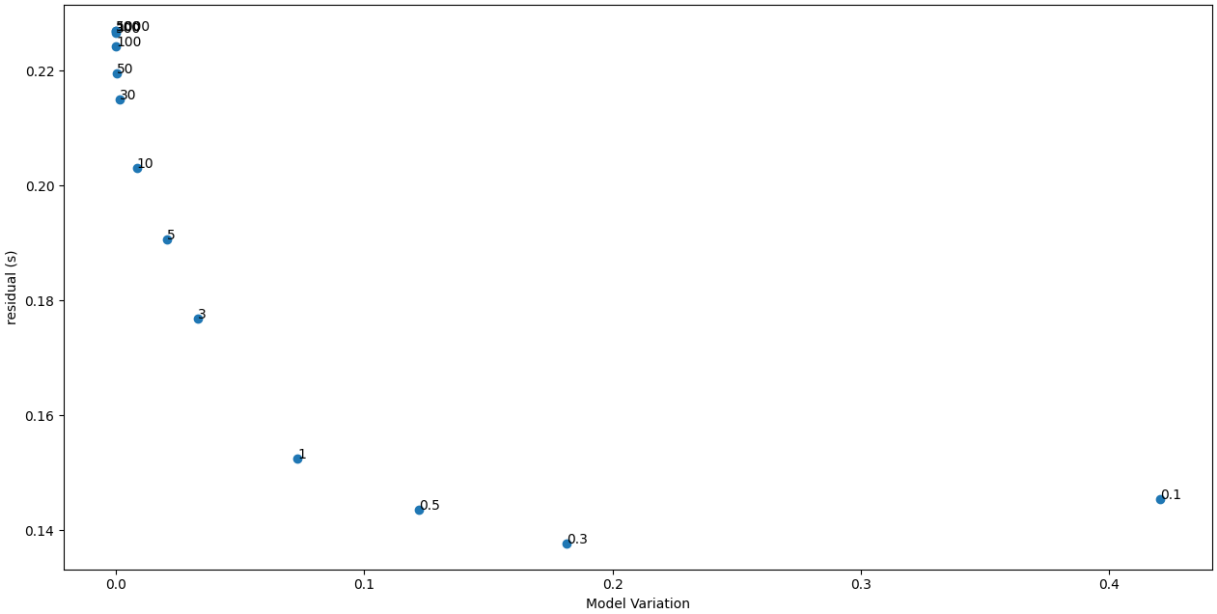


Figure S10. A trade-off curve (L-curve) showing the connection between the residual RMS and model variation for different norm damping values. A damping value of 10 was chosen because it lies at an inflection point of the curve and represents the best compromise between data misfit and model complexity.